

## Second plasmon and collective modes in binary Coulomb systems

G. J. KALMAN<sup>1</sup>, Z. DONKÓ<sup>1,2</sup>, P. HARTMANN<sup>1,2</sup> and K. I. GOLDEN<sup>3</sup>

<sup>1</sup> *Department of Physics, Boston College - Chestnut Hill, MA 02467, USA*

<sup>2</sup> *Institute for Solid State Physics and Optics, Wigner Research Centre for Physics, Hungarian Academy of Sciences H-1121 Budapest, Konkoly-Thege Miklós str. 29-33, Hungary*

<sup>3</sup> *Department of Mathematics and Statistics and Department of Physics, University of Vermont Burlington, VT 05405-1455, USA*

received 13 March 2014; accepted in final form 4 July 2014

published online 28 July 2014

PACS 52.27.Gr – Strongly-coupled plasmas

PACS 52.27.Cm – Multicomponent and negative-ion plasmas

PACS 52.35.Fp – Electrostatic waves and oscillations (*e.g.*, ion-acoustic waves)

**Abstract** – In a system consisting of two different charged species we identify the excitation of a second, low-frequency plasmon. At strong coupling the doublet of high-frequency (first) and low-frequency (second) plasmons replaces the single-plasmon excitation that prevails at weak coupling. We observe the formation of the second plasmon from the acoustic Goldstone-type mode associated with a short-range interaction as the range is extended to infinity.

Copyright © EPLA, 2014

The existence of plasmons in many-body systems interacting through a Coulomb potential (plasmas, electron gases, etc.) with a characteristic oscillation frequency, the plasma frequency  $\omega_p = \sqrt{4\pi Z^2 e^2 n/m}$  (with the symbols having their usual meaning) was first observed by Tonks and Langmuir [1]. Its theoretical analysis started with the work of Vlasov [2,3] who realized that the unique behavior of the Coulomb interaction required a novel theoretical approach. Landau's subsequent criticism [4] of some aspects of Vlasov's work led to a deeper understanding of the wave-particle interaction and the ensuing damping mechanism. The identification of the plasma oscillations as a collective excitation—in fact, the very idea of collective excitations and the notion of collective coordinates—is due to the pioneering series of works by Bohm, Gross and Pines [5–8]. It was also Bohm and Gross (BG) [5,6] who determined the eponymous  $k$ -dependent positive dispersion of the plasmon, caused by the random motion of the particles. Soon, however, it became clear that both the Vlasov treatment and the BG dispersion share an underlying theoretical foundation (which later was reformulated in many different guises [7,9–11] and has commonly become known as the Random Phase Approximation (RPA)) and are appropriate for weak coupling only. The appropriate parameters that characterize the coupling strength for classical systems are  $\Gamma = Z^2 e^2 / ak_B T$  and for quantum

systems  $r_s = a/a_B$  ( $a$  is the Wigner-Seitz radius,  $a_B$  the Bohr radius and  $T$  the temperature). Motivated by the case of the electron gas in metals where the condition  $r_s < 1$  is mildly violated, it was Singwi *et al.* [12] who have made the first serious attempts to study the effect of strong coupling on the properties of the plasmon. However, the first systematic and reliable analysis of this problem, primarily through Molecular-Dynamics (MD) computer simulation was done by Hansen *et al.* [13–16]; in particular in [16] the change of the BG behavior to a negative dispersion, the hallmark phenomenon of strong coupling, was verified, which was predicted and investigated by a number of workers [17–20] around the same time. A different theoretical approach, the Quasi-localized Charge Approximation (QLCA), geared for the study of strongly coupled Coulomb systems [21,22] combined with advanced MD computer simulations has led to a thorough investigation of the plasmon dispersion. Experimentally, the plasmon dispersion of the electron gas has been mapped in various condensed-matter situations at low or moderate coupling values; with the advent of complex (dusty) plasma experiments, the way to directly observing strongly coupled plasmon behavior in the laboratory has opened up.

Looking at the problem from a more general point of view, we focus first on a system governed by a short-range interaction (*e.g.* by a Yukawa potential,  $\varphi(r) \propto e^{-\kappa r}/r$ ).

Such a system exhibits three  $\omega(k \rightarrow 0) \sim k$  acoustic Goldstone-type excitations [23], one of which is a longitudinal mode. This, however, is not the case for a plasma with long-range (*i.e.*  $\kappa = 0$ ) Coulomb interaction. The fundamental work of Anderson [24] has shown that this zero-mass Goldstone boson acquires a mass to transform itself into the finite-mass longitudinal plasmon with  $\omega(k \rightarrow 0) = \omega_p$ . It has also been demonstrated by Lange [25] that the argument that associates the generation of a Goldstone boson with a broken symmetry fails for long-range interaction. Moreover, it turns out that, protected by the Kohn sum rule [26], the plasmon is an extremely robust excitation, unaffected by correlations, *i.e.*  $\Gamma$  and  $r_s$  independent.

The question we address now in this letter is: what happens then in a (three-dimensional) binary Coulomb system, composed of two species of different masses and charges? Choosing the Yukawa system again as a starting paradigm, we observe that the system now exhibits, in addition to the longitudinal acoustic mode, a longitudinal optic mode, which at  $k = 0$  has frequency  $\omega_*$  and is degenerate with its two transverse counterparts (cf. the corresponding discussion on the 2D system in [27]). Following Anderson's argument, we now expect that with the Coulomb interaction switched on, the acoustic excitation acquires a mass, *i.e.* develops a finite frequency, and becomes a new excitation  $\omega(k \rightarrow 0) = \omega_-$  which hence we refer to as the low-frequency second plasmon. It is less obvious what happens to the gapped longitudinal excitation at  $\omega_*$ . What we show below is that the Coulomb interaction lifts the longitudinal/transverse degeneracy and elevates the longitudinal gap frequency from  $\omega_*$  (while leaving the transverse excitation frequency at  $\omega_*$ ) to generate a second massive excitation, the high-frequency (first) plasmon at  $\omega(k \rightarrow 0) = \omega_+$ . While it is this scenario that is expected and verified below for strongly coupled systems, the weak-coupling theories [2,3,5-7] do not in fact, show this behavior at all. The well-known RPA dispersion relation provides a single finite-frequency plasmon, at the combination of the plasma frequencies of the individual components (see below, eq. (5)).

To analyze more rigorously the excitation spectrum of the strongly coupled system we consider a model of a three-dimensional strongly correlated binary Coulomb liquid (BIM — Binary Ionic Mixture), consisting of two kinds of, say, positively charged particles of charges  $Z_1e$  and  $Z_2e$ , masses  $m_1$  and  $m_2$ , and concentrations  $c \equiv c_1$  and  $c_2$ , respectively. The two ionic species are immersed in a rigid, neutralizing background. A great deal of work has already been devoted to investigating the properties of such a system in different dimensions [28-35]. The problem of how correlations affect the plasmon dispersion was first raised by Hansen *et al.* [16,23,36,37] and it was shown that correlations lift the plasmon frequency from its low coupling  $\omega_0$  value. In [36,37] the notion of the hydrodynamic plasma frequency  $\bar{\omega}$  (see below eq. (6)) was introduced, as a candidate for a second excitation. The issue was

reconsidered in [21,22] on the basis of the QLCA (see below), where a high-frequency and a low-frequency longitudinal and an additional transverse gapped modes were identified (cf. eq. (4) below). However, the full understanding and the full physical portrayal of these modes were lacking. While over the past decade the QLCA has been tested and corroborated on a number of Coulomb and Yukawa systems [38-41], no such data are available for binary systems. Thus, the excitation spectrum of binary Coulomb systems is still poorly understood. There is even less understanding of the transition from the weakly coupled to the strongly coupled regime. Here we attempt a full new analysis of the collective excitations of the system. Our main interest lies in the liquid state, but we will extend our investigation to the crystalline solid phase as well, primarily with the goal of establishing the link between the excitation spectra in the liquid and solid phases.

Our primary approach is to study the system by MD simulations. We accompany the simulations with a compact re-formulation of the QLCA. The combination of these two methods, whose results are in very good agreement, yields a full description and understanding of the hitherto unexplored and somewhat unexpected structure of the collective excitation spectrum of binary Coulomb systems. It also gives an insight into the link between this spectrum and the spectrum of a similar system with a short-range Yukawa interaction, see, *e.g.*, [42].

Our MD code is based on the Particle-Particle Particle-Mesh (PPPM) method [43], and uses  $N = 10000$  particles for the liquid-phase calculations, and somewhat different number of particles in the case of lattice configurations, to ensure the matching of the simulation box and a perfect (bcc or fcc) lattice. For liquid-phase conditions the initial positions of the particles are set randomly, for solid-phase simulations particles are set at lattice sites. In the measurement phase of the simulation, that comprises  $\sim 2.6 \times 10^6$  time steps, data are collected for the three pair correlation functions,  $g_{AB}(r)$ , as well as for the microscopic density and current fluctuations, for the two species. The Fourier transform yields from these data (see, *e.g.*, [15]) the dynamical partial structure functions,  $S_{AB}(k, \omega)$ , as well as the partial longitudinal and transverse current fluctuation spectra,  $L_{AB}(k, \omega)$  and  $T_{AB}(k, \omega)$ , respectively. Collective modes are identified as peaks appearing in these spectra. With the above number of simulation particles and the time covered by the simulations we obtain a good signal-to-noise ratio of the measured quantities, and a good resolution of the dynamical spectra over a wide range of the parameters, even at relatively low coupling, a domain that is less accessible computationally.

The QLCA is based on the premise that in the strongly coupled phase, particles are trapped in local potential minima and that the oscillation of these quasi-localized particles governs the formation of the collective modes. The dispersion of the modes is described in terms of the

dynamical matrix  $C$ :

$$\begin{aligned}
C_{AB}^{\mu\nu}(\mathbf{k}) &= -\frac{1}{4\pi} \int d^3\bar{\mathbf{r}} \{ \omega_{AB}^2 \psi^{\mu\nu}(\bar{\mathbf{r}}) e^{-i\mathbf{k}\cdot\bar{\mathbf{r}}} [1 + h_{AB}(r)] \\
&\quad - \delta_{AB} \sum_{C(all)} \Omega_{AC}^2 \psi^{\mu\nu}(\bar{\mathbf{r}}) [1 + h_{AC}(r)] \} \\
&\quad + \delta_{AB} \delta^{\mu\nu} \sum_{C(all)} \frac{1}{3} \Omega_{AC}^2, \\
\psi^{\mu\nu}(\bar{\mathbf{r}}) &= \frac{1}{\bar{r}^3} \left( 3 \frac{r^\mu r^\nu}{r^2} - \delta^{\mu\nu} \right) - \frac{4\pi}{3} \delta^{\mu\nu} \delta(\bar{\mathbf{r}}). \quad (1)
\end{aligned}$$

The indices  $A, B$  designate the species;  $h_{AB}(r)$  is the pair correlation function between particles in species  $A$  and  $B$ .

$$\begin{aligned}
\omega_{AB}^2 &= \frac{4\pi e^2 Z_A Z_B \sqrt{n_A n_B}}{\sqrt{m_A m_B}}, \\
\Omega_{AB}^2 &= \frac{4\pi e^2 Z_A Z_B n_B}{m_A} \quad (2)
\end{aligned}$$

are the nominal plasma and Einstein frequencies, respectively. In this letter we are interested in the longitudinal modes only, in particular their behavior at  $k = 0$ , where the salient features of the mode structure come into focus, and

$$\begin{aligned}
C_{11}^L(0) &= \omega_{11}^2 + \frac{1}{3} \Omega_{12}^2, & C_{22}^L(0) &= \omega_{22}^2 + \frac{1}{3} \Omega_{21}^2, \\
C_{12}^L(0) &= \frac{2}{3} \omega_{12}^2 = \frac{2}{3} \Omega_{12} \Omega_{21}; \\
C_{11}^T(0) &= \frac{1}{3} \Omega_{12}^2, & C_{22}^T(0) &= \frac{1}{3} \Omega_{21}^2, \\
C_{12}^T(0) &= -\frac{1}{3} \Omega_{12} \Omega_{21}, \quad (3)
\end{aligned}$$

The  $L$  and  $T$  superscripts designate longitudinal and transverse elements. The collective modes are obtained as the roots of the characteristic equation  $\|\mathbf{C} - \omega^2 \mathbf{I}\| = 0$ .

We introduce now the asymmetry parameters  $p$  and  $q$  with  $p^2 = Z_2 n_2 / Z_1 n_1$ , and  $q^2 = Z_2 m_1 / Z_1 m_2$ , and express all frequencies in the unit of  $\omega_1 \equiv \omega_{11} = \sqrt{4\pi Z_1^2 e^2 n_1 / m_1}$ , with  $Z = Z_2 / Z_1$  and  $m = m_2 / m_1$  for the charge and mass ratios, respectively. Now the resulting gap frequencies become

$$\begin{aligned}
\omega_{\pm}^2 &= \frac{1}{2} (B \pm \sqrt{\Delta}), \\
\omega_T^2 &\equiv \omega_*^2 = \frac{1}{3} (p^2 + q^2), \\
B &= 1 + p^2 q^2 + \frac{1}{3} (p^2 + q^2), \\
\Delta &= B^2 - \frac{4}{3} q^2 (1 + p^2)^2. \quad (4)
\end{aligned}$$

$\omega_+$  and  $\omega_-$  are the longitudinal plasmons, while  $\omega_T$  is a doubly degenerate gapped transverse mode. In addition we observe the appearance of the doubly degenerate transverse acoustic mode with a sound speed  $s$  of the order of  $s \sim \bar{\omega} a$  ( $\bar{\omega}$  is defined below). Note that the gap frequencies

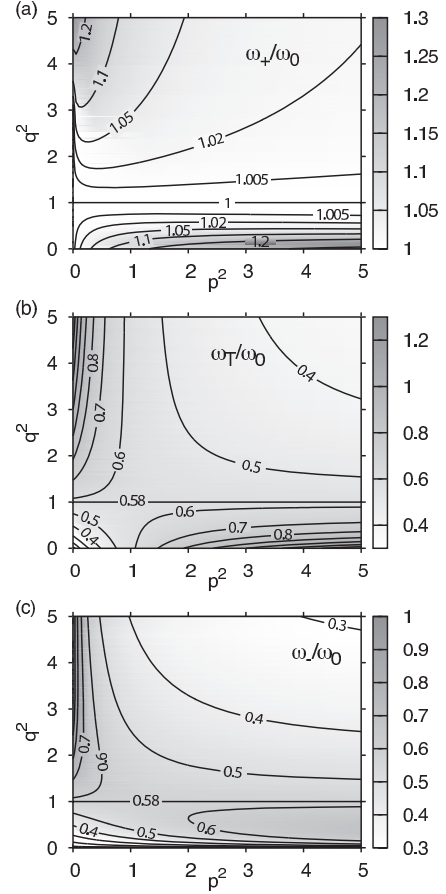


Fig. 1: Gap frequencies in relation to the RPA plasma frequency  $\omega_0 = \sqrt{1 + p^2 q^2}$ .

are ordered as  $\omega_+ > \omega_T > \omega_-$ . They satisfy a generalized Kohn sum rule [44], which, however, does not protect them from the unexpectedly complex dependence on the system parameters.

In the weak-coupling approximation (RPA), as already noted, there would exist only one excitation frequency,

$$\omega_0 = \sqrt{\omega_{p1}^2 + \omega_{p2}^2} = \sqrt{1 + p^2 q^2}. \quad (5)$$

The hydrodynamic (or virtual average atom) frequency [27] introduced by Hansen *et al.* [45] is

$$\bar{\omega} = \sqrt{q^2 / (p^2 + q^2)} (1 + p^2). \quad (6)$$

While this frequency plays a role in the low-frequency acoustic spectrum of the system (similarly to Yukawa systems [27]), it is not part of the spectrum displayed above. In fig. 1 we portray the three predicted gap frequencies in relation to the RPA plasma frequency  $\omega_0$ , showing the remarkable differences brought about by the strong coupling. The special role of the  $q = 1$  structure is visible as an  $\omega_+ = 1$ ,  $\omega_- = \omega_T = 1/\sqrt{3}$ ,  $p$ -independent separatrix, representing a quasi-one-component behavior [16,22,27,36,45,46].

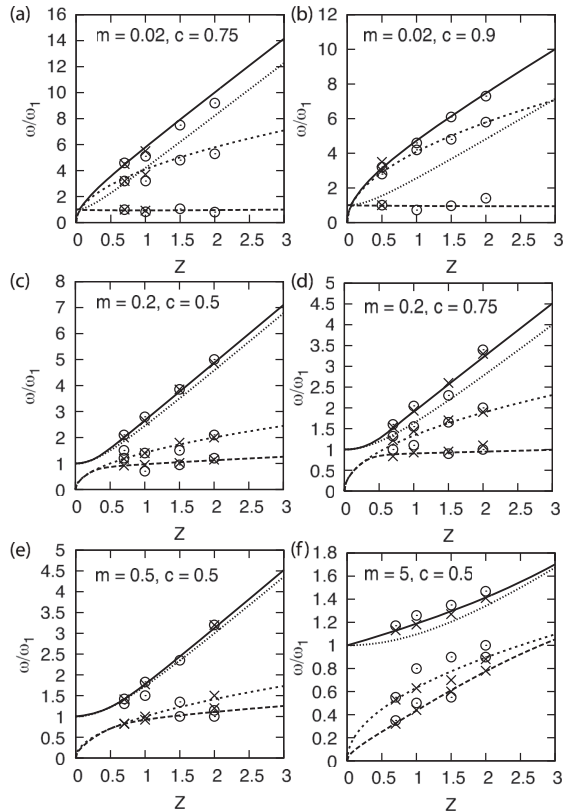


Fig. 2:  $Z$  and  $m$  dependences of the gap frequencies (lines) together with MD results for solid (crosses) and strongly coupled liquid (circles) cases. Parameters are indicated in the panels.

In the following sequence of graphs we compare the QLCA predictions with the behavior of the system determined by MD simulations over a range of coupling values. We characterize the strength of the overall coupling by the value of  $\Gamma \equiv \Gamma_1 = Z_1 e^2 / a_1 k_B T$ , where  $a_A^3 = 3 / (4\pi n_A)$ .

Depending on  $Z_2$  and  $c_2$ , the actual coupling strength can be quite different. A fair measure of its value can be gleaned by observing where the freezing of the liquid sets on. We have found that defining  $\Gamma_{\text{eff}} = \langle Z \rangle^2 e^2 / (a_0 k_B T_0) = c^{5/3} (1 + p^2)^2 \Gamma$  provides a reasonably uniform liquid/solid phase boundary at  $\Gamma_{\text{eff}} \approx 174$ , where  $\langle Z \rangle = (Z_1 n_1 + Z_2 n_2) / (n_1 + n_2)$ ,  $T_0$  is the temperature, and  $a_0$  is the Wigner-Seitz radius calculated from the total density  $n_1 + n_2$ . Our  $\Gamma$  values range from weak/moderate coupling ( $\Gamma = 1$ ) moving up into and beyond the crystallization regime ( $\Gamma > 150$ ). For the lattice structure in the solid phase, for  $c = 0.5$  we expect the lattice structure to be bcc, for  $c = 0.75$  to be fcc. The stability of these lattices at zero temperature has been tested: for the bcc  $0.278 < Z < 3.596$ , for the fcc  $0.731 < Z < 1.512$ .

In fig. 2 the predicted  $Z$  and  $m$  dependences of the gap frequencies are shown for different concentrations along with MD simulation results for high  $\Gamma$  values. Shown are also the matching of the liquid gap frequencies with the

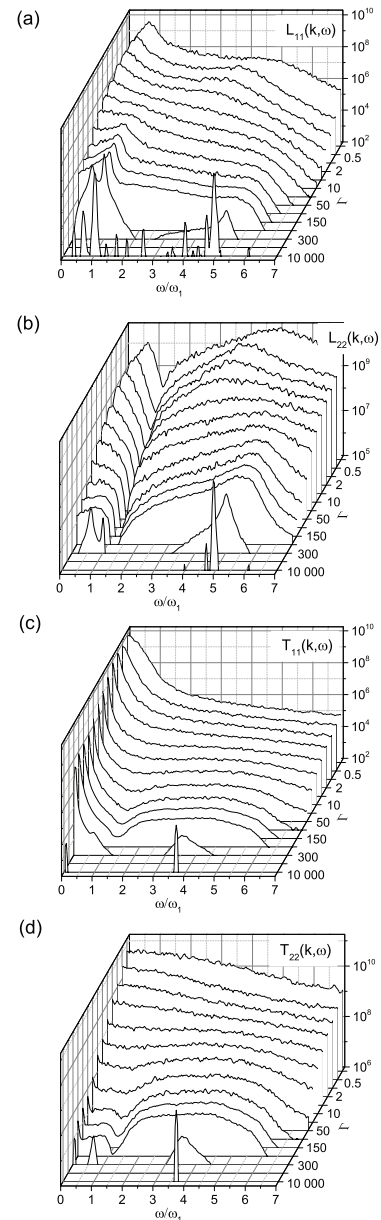


Fig. 3: Dynamical partial structure functions for a series of coupling parameters  $\Gamma$  for  $Z = 0.8$ ,  $m = 0.02$ ,  $c = 0.75$  and the lowest wave number accessible in the simulation:  $ka = 0.188$ , where  $a = \sqrt{a_1 a_2}$ . The two spectra in the front represent solid (fcc) systems with  $\Gamma = 10000$  and  $300$ , respectively.

corresponding values in the crystalline solid. In the bcc there is a one-to-one agreement between the liquid and solid gap frequencies; in the fcc there are additional optic modes, due to the increased number of particles inside the unit cell (cf. [27]). The overall agreement with the theoretical prediction is very good: the analytic description of the mode structure seems to be well confirmed.

It should be emphasized that the QLCA gap frequencies are formally  $\Gamma$  independent and the detailed structure of the correlation functions does not enter eqs. (5). (This is

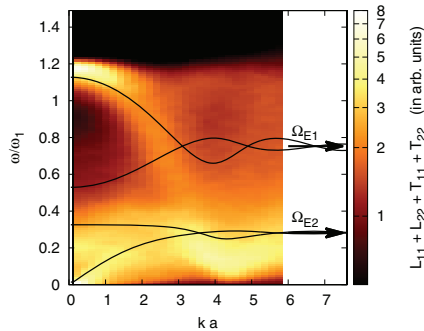


Fig. 4: (Color online) Color map in the background is the sum of current fluctuation spectra,  $L_{11} + L_{22} + T_{11} + T_{22}$ , from MD simulations for  $Z = 0.7$ ,  $m = 5$ ,  $c = 0.5$ , and  $\Gamma = 100$ . The black lines overlaid are dispersions relations for the same system computed by QLCA.

not true for the  $k \neq 0$  behavior, not shown here.) The only feature that has been exploited is that  $g_{AB}(r = 0) = 0$ ; nevertheless the strong-coupling approximation is inherent in the model, because the QLCA is built on the localization assumption, a hallmark of the strong coupling.

More insight into how strong coupling affects the dynamics of the system can be gleaned from fig. 3, where we show the dynamical partial structure functions  $L_{11}(\omega)$ ,  $L_{22}(\omega)$ ,  $T_{11}(\omega)$ ,  $T_{22}(\omega)$ ,  $L(\omega)$  representing the spectra of the longitudinal,  $T(\omega)$  of the transverse current fluctuations. We present sequences of graphs for a selected set of parameters where the effect of the increasing strength of the coupling can be followed, from low coupling ( $\Gamma = 0.2$ ) into well in the crystalline phase. We observe that at low  $\Gamma$  values the system exhibits RPA behavior, where only one gapped mode  $\omega_0$  survives. The characteristic strong-coupling behavior with the appearance of the  $\omega_+$  first plasmon and the  $\omega_-$  second plasmon takes place around  $\Gamma = 40$ , while the transverse modes appear later, around  $\Gamma = 100$ . (Note, however, that these  $\Gamma$  values are appropriate for the chosen system parameters only, and they vary with the change of the system parameters.) There seems to be a “no-man’s land”, somewhere between  $\Gamma = 10$  and  $\Gamma = 40$ , where virtually no collective excitation exists. A remarkable feature can be observed in the  $L_{22}(\omega)$  (2 is the light component) graph: the development of a very well defined Fano-like sharp minimum, at an  $\omega$  value adjacent to  $\omega_-$ ; a somewhat similar feature in the response (rather than in the equilibrium fluctuation spectrum) of an electron-ion plasma has been reported by Murillo [47]. A discussion and attempted explanation of this phenomenon will be presented elsewhere [48].

While the focus of this letter is a presentation and discussion of the  $k = 0$  gapped excitations, it is instructive to examine a sample of the full  $\omega(k)$  dispersions. This is done in fig. 4, where for a representative set of parameters the MD result is portrayed for the liquid phase, accompanied by theoretical dispersion curves calculated with the aid of the QLCA. We observe the appearance of the acoustic

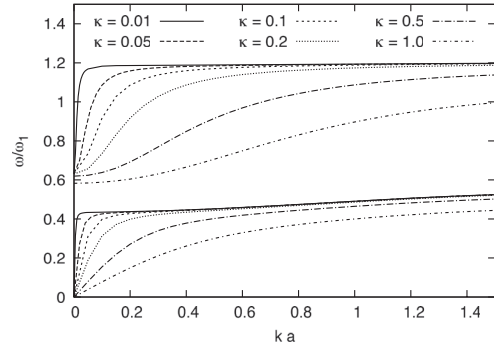


Fig. 5: Longitudinal dispersion curves calculated for binary Yukawa bcc lattices for a series of  $\kappa = a/\lambda_D$  and  $Z = 1$ ,  $m = 5$ .

doubly degenerate transverse mode with a sound speed  $s$  of the order of  $s \sim \bar{\omega}a$ . We also note the two  $\omega(k \rightarrow \infty)$  actual Einstein frequencies, which can be calculated to be

$$\Omega_{E1}^2 = \frac{1}{3}(\omega_{11}^2 + \Omega_{12}^2), \quad \Omega_{E2}^2 = \frac{1}{3}(\omega_{22}^2 + \Omega_{21}^2). \quad (7)$$

Finally, it is instructive to explore the details of the transition from a Yukawa system with  $\kappa \neq 0$  to the singular Coulomb ( $\kappa = 0$ ) case. A sequence of dispersion curves illustrating the process as described in the introductory paragraph is given in fig. 5. While the transition is discontinuous at  $k = 0$ , it becomes quasi-continuous in the  $k > \kappa$  domain.

In summary, we have shown that in the strongly coupled phase of a binary system of charged particles the excitation spectrum of collective modes dramatically changes from the simple structure that exists in the domain of weak coupling: the single plasmon with the combined plasma frequency  $\omega_0$  of the two species  $\omega_0 = \sqrt{\omega_{p1}^2 + \omega_{p2}^2}$  is replaced by the doublet of a new type of excitations, a high-frequency first plasmon  $\omega_+$  and a low-frequency, second plasmon  $\omega_-$ . This second plasmon is generated by the Anderson mechanism from the longitudinal acoustic Goldstone boson that one would have in a system with a short-range interaction. There is, however, no smooth transition from the weak coupling  $\omega_0$  to the strong coupling  $\omega_+$ . In the intermediate coupling domain no collective excitation can be discerned.

As to the remaining part of the spectrum, we have confirmed the existence of transverse excitations, consisting of a set of doubly degenerate acoustic modes and a set of doubly degenerate gapped modes. The acoustic speed is governed by the oscillation frequency of the “virtual atom” [27] (hydrodynamic frequency [45]).

The physical systems that come closest to the realization of the simplified model investigated in this paper are brown dwarf interiors [49,50], carbon-oxygen stars in their helium shell burning phase [37,51], and trapped  $\text{Be}^+ \text{-Xe}^{+44}$  ionic mixtures [30], as well as mixtures of fermion gases, such as those constituted by electrons in transition metals [52] and in heavy-fermion systems [53].

\* \* \*

This work has been supported by the NSF Grants 0715227, 0813153, 1105005, 0812956, OTKA Grants K-105476 and NN-103150.

## REFERENCES

- [1] TONKS L. and LANGMUIR I., *Phys. Rev.*, **33** (1929) 195.  
 [2] VLASOV A. A., *J. Exp. Theor. Phys.*, **8** (1938) 291 (in Russian).  
 [3] VLASOV A. A., *Sov. Phys. Usp.*, **10** (1968) 721.  
 [4] LANDAU L., *J. Phys. USSR*, **10** (1946) 25 (English translation in *JETP*, **16** (1963) 574); reproduced in *Collected papers of L. D. Landau*, edited and with an introduction by TER HAAR D. (Pergamon Press) 1965, pp. 445–460; and in *Men of Physics: L. D. Landau*, edited by TER HAAR D., Vol. **2** (Pergamon Press) 1965.  
 [5] BOHM D. and GROSS E. P., *Phys. Rev.*, **75** (1949) 1851.  
 [6] BOHM D. and GROSS E. P., *Phys. Rev.*, **75** (1949) 1864.  
 [7] PINES D. and BOHM D., *Phys. Rev.*, **85** (1952) 338.  
 [8] BOHM D. and PINES D., *Phys. Rev.*, **92** (1953) 609.  
 [9] NOZIÈRES P. and PINES D., *Phys. Rev.*, **109** (1958) 741.  
 [10] GELL-MANN M. and BRUECKNER K. A., *Phys. Rev.*, **106** (1957) 364.  
 [11] SAWADA K., BRUECKNER K. A., FUKUDA N. and BROUT R., *Phys. Rev.*, **108** (1957) 507.  
 [12] SINGWI K. S., TOSI M. P., LAND R. H. and SJÖLANDER A., *Phys. Rev.*, **176** (1968) 589.  
 [13] POLLOCK E. L. and HANSEN J. P., *Phys. Rev. A*, **8** (1973) 3110.  
 [14] HANSEN J. P., *Phys. Rev. A*, **8** (1973) 3096.  
 [15] HANSEN J. P., McDONALD I. R. and POLLOCK E. L., *Phys. Rev. A*, **11** (1975) 1025.  
 [16] HANSEN J. P., McDONALD I. R. and VIEILLEFOSSE P., *Phys. Rev. A*, **20** (1979) 2590.  
 [17] KALMAN G., KEMPA K. and MINELLA M., *Phys. Rev. B*, **43** (1991) 14238.  
 [18] VOM FELDE A., SPRÖSSER-PROU J. and FINK J., *Phys. Rev. B*, **40** (1989) 10181.  
 [19] SINGWI K., SJÖLANDER A., TOSI M. and LAND R., *Solid State Commun.*, **7** (1969) 1503.  
 [20] VASHISHTA P. and SINGWI K. S., *Phys. Rev. B*, **6** (1972) 875.  
 [21] KALMAN G. and GOLDEN K. I., *Phys. Rev. A*, **41** (1990) 5516.  
 [22] GOLDEN K. I. and KALMAN G. J., *Phys. Plasmas*, **7** (2000) 14.  
 [23] LANDAU L. D. and LIFSCHITZ E. M., *Statistical Physics* (Pergamon Press) 1980.  
 [24] ANDERSON P. W., *Phys. Rev.*, **130** (1963) 439.  
 [25] LANGE R. V., *Phys. Rev. Lett.*, **14** (1965) 3.  
 [26] BROUT R., *Phys. Rev.*, **113** (1959) 43.  
 [27] KALMAN G. J., HARTMANN P., DONKÓ Z., GOLDEN K. I. and KYRKOS S., *Phys. Rev. E*, **87** (2013) 043103.  
 [28] HANSEN J. P., TORRIE G. M. and VIEILLEFOSSE P., *Phys. Rev. A*, **16** (1977) 2153.  
 [29] IGARASHI T. and IYETOMI H., *J. Phys. A: Math. Gen.*, **36** (2003) 6197.  
 [30] DEWITT H. E. and SLATTERY W. L., in *Proceedings of Strongly Coupled Coulomb Systems*, edited by KALMAN G., ROMMEL J. and BLAGOEV K. (Plenum Press, New York) 1998, pp. 1–7.  
 [31] BAUS M. and HANSEN J.-P., *Phys. Rep.*, **59** (1980) 1.  
 [32] BASTEA S., *Phys. Rev. E*, **71** (2005) 056405.  
 [33] DALIGAULT J., *Phys. Rev. Lett.*, **108** (2012) 225004.  
 [34] FERREIRA W. P., CARVALHO J. C. N., OLIVEIRA P. W. S., FARIAS G. A. and PEETERS F. M., *Phys. Rev. B*, **77** (2008) 014112.  
 [35] FERREIRA W. P., FARIAS G. A. and PEETERS F. M., *J. Phys.: Condens. Matter*, **22** (2010) 285103.  
 [36] BAUS M., *Phys. Rev. Lett.*, **40** (1978) 793.  
 [37] CANAL R., ISERN J. and LABAY J., *Astrophys. J.*, **241** (1980) L33.  
 [38] HARTMANN P., DONKÓ Z., KALMAN G. J., KYRKOS S., GOLDEN K. I. and ROSENBERG M., *Phys. Rev. Lett.*, **103** (2009) 245002.  
 [39] HOU L.-J., MIŠKOVIĆ Z. L., PIEL A. and MURILLO M. S., *Phys. Rev. E*, **79** (2009) 046412.  
 [40] PIEL A., NOSENKO V. and GOREE J., *Phys. Plasmas*, **13** (2006) 042104.  
 [41] KÄHLERT H., KALMAN G. J. and BONITZ M., *Dynamics of strongly correlated and strongly inhomogeneous plasmas*, to be published in *Phys. Rev. E*.  
 [42] DONKÓ Z., KALMAN G. J. and HARTMANN P., *J. Phys.: Condens. Matter*, **20** (2008) 413101.  
 [43] HOCKNEY R. and EASTWOOD J., *Computer Simulation Using Particles* (Taylor & Francis) 2010.  
 [44] KALMAN G. J. and KÄHLERT H., in preparation.  
 [45] HANSEN J., JOLY F. and McDONALD I., *Physica A: Stat. Mech. Appl.*, **132** (1985) 472.  
 [46] GOLDEN K. I., GREEN F. and NEILSON D., *Phys. Rev. A*, **32** (1985) 1669.  
 [47] MURILLO M. S., *Phys. Rev. E*, **81** (2010) 036403.  
 [48] SILVESTRI L., KALMAN G. J., DONKÓ Z., HARTMANN P. and KÄHLERT H., arXiv:1404.1661 [physics.plasm-ph] (2014).  
 [49] SLATTERY W. L., DOOLEN G. D. and DEWITT H. E., *Phys. Rev. A*, **26** (1982) 2255.  
 [50] DEWITT H. E., *Strongly coupled ionic mixtures and the h/he eos*, in *Proceedings of The Equation of State in Astrophysics: IAU Colloquium 147*, edited by CHABRIER G. and SCHATZMAN E. (Cambridge University Press, Cambridge, UK) 1994, p. 330.  
 [51] TRIMBLE V., *Rev. Mod. Phys.*, **54** (1982) 1183.  
 [52] CHAKRABORTY T., *Phys. Rev. B*, **29** (1984) 3975.  
 [53] MILLIS A. J., LAVAGNA M. and LEE P. A., *Phys. Rev. B*, **36** (1987) 864.